

The *orf13* T-DNA Gene of *Agrobacterium rhizogenes* Confers Meristematic Competence to Differentiated Cells¹

Pia A. Stieger², Alain D. Meyer³, Petra Kathmann, Corinne Fründt⁴, Isabel Niederhauser, Mario Barone, and Cris Kuhlemeier*

Institute of Plant Sciences, University of Bern, CH-3013 Bern, Switzerland (P.A.S., P.K., I.N., M.B., C.K.); Institut des Sciences Végétales, Centre National de la Recherche Scientifique, 91198 Gif-sur-Yvette, France (A.D.M.); and Friedrich Miescher Institut, CH-4058 Basel, Switzerland (C.F.)

Plant infections by the soil bacterium *Agrobacterium rhizogenes* result in neoplastic disease with the formation of hairy roots at the site of infection. Expression of a set of oncogenes residing on the stably integrated T-DNA is responsible for the disease symptoms. Besides the *rol* (root locus) genes, which are essential for the formation of hairy roots, the open reading frame *orf13* mediates cytokinin-like effects, suggesting an interaction with hormone signaling pathways. Here we show that ORF13 induced ectopic expression of KNOX (KNOTTED1-like homeobox) class transcription factors, as well as of several genes involved in cell cycle control in tomato (*Lycopersicon esculentum*). ORF13 has a retinoblastoma (RB)-binding motif and interacted with maize (*Zea mays*) RB in vitro, whereas ORF13, bearing a point mutation in the RB-binding motif (ORF13*), did not. Increased cell divisions in the vegetative shoot apical meristem and accelerated formation of leaf primordia were observed in plants expressing *orf13*, whereas the expression of *orf13** had no influence on cell division rates in the shoot apical meristem, suggesting a role of RB in the regulation of the cell cycle in meristematic tissues. On the other hand, ectopic expression of *LeT6* was not dependent on a functional RB-binding motif. Hormone homeostasis was only altered in explants of leaves, whereas in the root no effects were observed. We suggest that ORF13 confers meristematic competence to cells infected by *A. rhizogenes* by inducing the expression of KNOX genes and promotes the transition of infected cells from the G1 to the S phase by binding to RB.

Plant pathogens change the differentiation program of plant cells to create a protected surrounding with nutrient availability. *Agrobacterium tumefaciens* and *Agrobacterium rhizogenes* infect wounds of several dicotyledonous and some monocotyledonous species and thereby generate tumorous outgrowths at the site of infection (Nilsson and Olsson, 1997). The genes required for tumorigenesis are found on extrachromosomal elements (Ti plasmids for *A. tumefaciens* and Ri plasmids for *A. rhizogenes*), of which a portion (T-DNA) is integrated into the plant genome (Zhu et al., 2000; Zupan et al., 2000). Both pathogens are able to respecify differentiated cells to gain meristematic functions and, in the case of *A. rhizogenes*, infections are characterized by a massive production of adventitious roots (Meyer et al., 2000). Root prolifer-

ation is not due to diffusible cell division factors and a direct interaction of the proteins encoded on the T-DNA with plant hormonal metabolism could not be shown. The T-DNA encodes up to 18 open reading frames, depending on the bacterial strain (Slightom et al., 1986). Insertional mutagenesis showed that insertions in only 4 of the potential 18 loci noticeably affected the morphology of the hairy roots that were produced (White et al., 1985). These loci were named root locus A-D (*rolA-D*).

In addition to the *rol* genes, *orf13* is encoded on the T-DNA of *A. rhizogenes*. The sequence of *orf13* is highly conserved in the agropine-, mannopine-, cucumopine-, and mikimopine-type Ri plasmids, and two plant counterparts were found in tobacco (*Nicotiana tabacum* [*torf13*]) and in tree tobacco (*Nicotiana glauca* [NgORF13]; Aoki et al., 1994; Fründt et al., 1998). Expression of *orf13* under the control of the cauliflower mosaic virus 35S promoter in transgenic tobacco plants causes severe alterations in morphogenesis and development, such as leaf wrinkling, shortened but very variable internode length, asymmetric flowers, and a poorly developed root system (Hansen et al., 1993; Lemcke and Schmölling, 1998). Similar morphological changes are observed in plants with elevated cytokinin levels (Medford et al., 1989). Nevertheless, no increase in cytokinin production was observed in *orf13*-expressing tobacco plants (Lemcke and Schmölling, 1998).

¹ This work was supported by a Marie-Heim-Vögtlin fellowship (SNF 31-55540.98, EU QLK5-CT-2000-00357, and SNF-TMR 83 EU-050209 to P.A.S.).

² Present address: Physiologie Végétale University of Neuchâtel, Rue Emile Argand 13, CH-2007 Neuchâtel, Switzerland.

³ Present address: Advolis Life Science Concepts, Oetlingerstrasse 10, CH-4057 Basel, Switzerland.

⁴ Present address: Novartis Pharma AG, CH-4002 Basel, Switzerland.

* Corresponding author; e-mail cris.kuhlemeier@ips.unibe.ch; fax 41-31-631-49-42.

Article, publication date, and citation information can be found at www.plantphysiol.org/cgi/doi/10.1104/pp.104.040899.

Besides hormonal actions of the ORF13 protein in plants, an influence on cell proliferation has been reported. Carrot discs inoculated with *Agrobacterium* carrying 35S::orf13 developed dark green callus (Fründt et al., 1998). Furthermore, endoreduplication was reduced in 35S::orf13 plants (Meyer et al., 2000), indicating an interaction of ORF13 with cell cycle control. Analysis of the ORF13 protein sequence revealed the retinoblastoma (RB)-binding motif LxCxE (Meyer et al., 2000). The LxCxE motif was shown for D-type cyclins and several oncoproteins to interact with C(706) in the retinoblastoma protein (RB; Horowitz et al., 1989; Kaelin et al., 1990; Weinberg, 1995). This motif was found in all members of the ORF13 family, i.e. in the agropine-, mannopine-, cucumopine-, and mikimopine-type Ri plasmids, including the two cloned plant counterparts of ORF13 in tobacco (torf13) and tree tobacco (NgORF13), suggesting a function for this conserved domain. The function of the RB in regulating the transition from G1 to the S phase in the cell cycle has been characterized intensively for mammals (Weinberg, 1995). It is also present in other eukaryotic systems, such as *Drosophila* (Du et al., 1996) and plants (Murray, 1997). Cloning and expression studies of several genes of the cyclinD/RB/E2F pathway in plants allow us to draw some parallels between plants and animals (Mironov et al., 1999).

Orf13 expression leads to the formation of spikes (protrusions between minor veins) on leaves and petals of tobacco (Meyer et al., 2000). Similar structures are formed on leaves, when KNOX (KNOTTED1-like homeobox) genes are overexpressed (Sinha et al., 1993; Chuck et al., 1996; Sentoku et al., 2000). KNOX genes can be grouped into two classes. Class I homeobox genes are preferentially expressed in shoot and floral meristems, whereas class II homeobox genes have much wider expression domains, suggesting functions outside of meristem development. Plants with increased levels of cytokinins, ectopic expression of KNOX genes, or ectopic expression of D-class cyclins share similarities in their phenotype. Plants are dwarfs, their leaf area is reduced, and leaves are wrinkled with knots on the leaf surface (Medford et al., 1989; Estruch et al., 1991; Chuck et al., 1996; Dewitte et al., 2003). In addition, elevated levels of cytokinin lead to ectopic expression of the KNOX genes *STM* and *KNAT1* (Rupp et al., 1999), just as ectopic expression of KNOX-class genes leads to elevated cytokinin contents in the shoot (Kusaba et al., 1998; Hewelt et al., 2000; Frugis et al., 2001). In contrast, *cyclinD*-overexpressing plants have normal levels of cytokinins and show no increase in the expression of KNOX genes (Riou-Khamlichi et al., 1999; Dewitte et al., 2003). Thus, cytokinins, KNOX-class genes, and D-type cyclins may partially act in a common pathway with D-type cyclins acting downstream of KNOX genes and cytokinins. Since *orf13*-expressing tobacco plants manifest similarities with the phenotypes described for cytokinin-overproducing plants, as well as with plants ectopically

expressing KNOX-class genes or the *cyclinD3.1* gene, ORF13 may interfere with cell differentiation by acting on a pathway influencing cytokinin signaling, as well as KNOX-class gene and D-type cyclin gene expression at the same time.

This study aims to characterize the effect of *orf13* expression on cell cycle control and KNOX expression in plants expressing *orf13* ectopically. The function of the RB-binding motif LxCxE in the ORF13 protein was analyzed. For that reason, the *orf13* gene with a point mutation in the RB-binding site was ectopically expressed in plants and the plant phenotype was compared to plants expressing the nonmutated *orf13* gene. In our study, we have chosen tomato (*Lycopersicon esculentum*) plants, because the meristem is easily accessible and leaf form is compound. Furthermore, the function of the KNOX genes in leaf formation is well described in tomato (Hareven et al., 1996; Chen et al., 1997).

RESULTS

The ORF13 Protein Binds to the RB via the LxCxE Motif In Vitro

To address the question of whether ORF13 is capable of physical interaction with the cell cycle regulating RB, the LxCxE motif of the mannopine-type pRi8196 was changed into LxAxK via site-directed mutagenesis. Both versions were expressed in *Escherichia coli* as recombinant proteins with 6-His tags and assayed for copurification in pull-down experiments with recombinant human glutathione S-transferase (GST)-RB fusions attached to glutathione Sepharose beads. The binding assay (Fig. 1) showed that the ORF13 protein with a native LxCxE sequence (ORF13) could bind to pRb with an intact C(706), but not to the pRb mutated in C(706), pRb(C706F). ORF13 harboring the LxAxK motif (ORF13*) was unable to bind pRb in this assay, indicating that the LxCxE motif in pORF13 is functional and that the pORF13-pRb interaction depends on the same C(706) in pRb as for D-type cyclins and adenoviral oncoproteins (Fig. 1).

Effect of the Functional RB-Binding Motif in ORF13 on Plant Development

To test the hypothesis that phenotypic alterations in *orf13*-expressing plants were due to the interaction of ORF13 with RB, either the *orf13* gene with the LxCxE RB-binding motif (*orf13*) or the *orf13* gene with the LxAxK motif (*orf13**), both driven by the cauliflower mosaic virus 35S promoter, were introduced into tomato plants. Six independently transformed lines with comparable phenotypes were obtained for *orf13* and five independently transformed lines with comparable phenotypes were obtained for *orf13**. Two lines of each (L1 and L2) were used for further investigation. *Orf13*-expressing plants had a reduced growth in

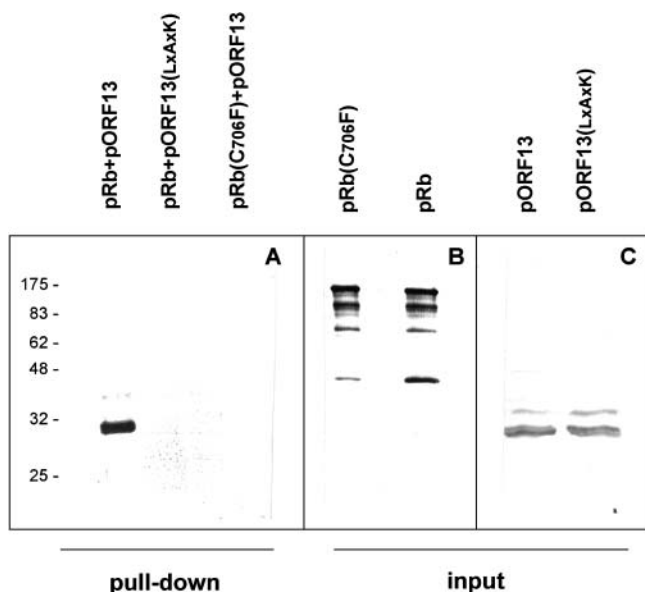


Figure 1. In vitro interaction of the recombinant ORF13-encoded protein (pORF13) with recombinant human pRb. The interaction depends on the presence of the LxCxE motif in pORF13 and on the C(706) in pRb. A, Pull-down assay. GST-RB and GST-RB(C706F) bound to glutathione beads were incubated with 6-His pORF13 and 6-His pORF13 (LxAxK). Only the combination where the interaction motif is intact in both protein partners allowed purification of the complex. B and C, Input controls. Aliquots of the recombinant proteins were loaded before the assay for interaction. A and C, Blots are decorated with monoclonal anti-6-His antibodies; B, blot with monoclonal anti-human RB antibodies. The sizes of the molecular mass markers are indicated on the left.

height and developed fewer leaves before entering the reproductive stage (Table I; Fig. 2A). Flowering was advanced. In control plants, lateral branch outgrowth was first observed at the time of flower induction. However, in *orf13*-expressing plants, the apical dominance was lost before the onset of flowering and the rate of lateral branch development was increased (Table I). Also *orf13** plants had stunted growth and a reduced apical dominance, comparable to *orf13* plants, whereas the number of leaves formed before flowering and the flowering time of *orf13** plants were comparable to controls and differed from *orf13* plants (Table I).

Leaf size was reduced in *orf13*-expressing plants, but the size of leaf epidermal cells was unchanged (Fig. 2B; Table I). On the adaxial side of leaves, the formation of spikes was observed (Fig. 2D; Table I). Transverse sections of leaves were made at the site of spike formation (Fig. 2, L–N). In leaf spikes, the palisade parenchyma consisted of multiple cell layers with small isodiametric cells (Fig. 2, M and N), whereas in control leaves the palisade parenchyma consisted of one cell layer with elongated cells (Fig. 2L). Spikes frequently formed also on sepals, petals, and fruits. Sepal and petal numbers were increased in *orf13* plants

(Fig. 2, I and J; Fig. 3, A and B). Also, *orf13** plants formed spikes on leaves, sepals, petals, and fruits (Table I), but *orf13** expression had no influence on leaf size (Fig. 2B; Table I), as well as on sepal and petal numbers (Fig. 2K; Fig. 3, A and B).

Shoot architecture of *orf13*-expressing plants differed from wild type. Phyllotaxis was occasionally changed from spiral to irregular (data not shown). Leaves were often wrinkled, and the arrangement of lateral and intercalary leaflets was changed (Fig. 2, B, C, and F). The terminal leaflet was occasionally replaced by an outgrowth of the rachis (Fig. 2, B and E). Stems and petioles were frequently fasciated and petioles were fused to the main stem (Fig. 2, G and H). Whereas phyllotaxis and the arrangement of lateral and intercalary leaflets were normal in *orf13** plants (Fig. 2B), organ fasciation and fusion were also observed (data not shown).

In contrast to the shoot, ORF13 had only minor effects on root growth. Whereas root length was not significantly different between *orf13*-expressing and control plants, the dry weight was slightly reduced when *orf13* was expressed. Furthermore, root structure was similar to control plants. *Orf13** expression had no effect on root growth (data not shown).

The differences obtained in organ numbers and organ size in *orf13* but not in *orf13** plants compared to controls indicate that the interaction of ORF13 with RB had an influence on plant growth. On the other hand, shoot morphology and architecture seem to be altered in a non-RB-dependent way, since no difference between *orf13* and *orf13** plants was observed. Thus ORF13 had RB-dependent, but also RB-independent, effects on plant growth and development.

Morphological changes observed in plants expressing *orf13* were similar to changes in tobacco caused by elevated cytokinin levels (Medford et al., 1989; Estruch et al., 1991), but also similar to *diageotropica* tomato mutant plants, which are affected in auxin perception and signaling (Zobel, 1974; Kelly and Bradford, 1986). It is therefore possible that ORF13 interferes with the signal transduction pathway or the homeostasis of auxins and/or cytokinins. On the other hand, a cytokinin-like phenotype was also observed in Arabidopsis plants with ectopic expression of *cyclinD3* (Riou-Khamlichi et al., 1999), and the effects of *orf13* expression on plant growth might be linked to a change in cell cycle regulation.

Hormone Homeostasis

Several bioassays were carried out to characterize the effects of *orf13* expression on cytokinin and auxin homeostasis. Root growth and lateral root formation are known to depend on auxin (Davies, 1995). Whereas root growth is inhibited by auxin, the formation of lateral root primordia is stimulated (Celenza et al., 1995; Reed et al., 1998). Root growth and lateral root initiation were not significantly changed in *orf13* plants, and the addition of auxin to the growth

Table I. Phenotypic features of tomato plants expressing the *A. rhizogenes* gene *orf13*

The size of plants was measured 61 d after sowing. Leaves were counted that had formed on the main shoot before the first flower had developed. For flowering, days between sowing and the opening of the first flower were counted. Forty-nine days after sowing, branches were counted that had formed three or more leaves. The number of spikes was counted on the fifth and sixth leaf from the bottom 30 d after sowing. Leaf size was measured of the third leaf from the bottom 4 weeks after sowing and epidermis cells of the adaxial leaf side were visualized with an SEM and cells were counted. All values were compared with values for the wild type using a one-tailed Student's *t* test.

	Wild Type	ORF13L1	ORF13L2	ORF13*L1	ORF13*L2	Plants
						<i>n</i>
Growth (cm at day 61)	90.3±0.4	62.3±9.4 ^a	71.3±6.2 ^a	76.9±5.9 ^a	63.3±7.1 ^a	10
Leaves to first inflorescence	10±0.7	7.8±0.8 ^a	8.1±0.6 ^a	10.9±1.1	10.0±0.47	10
Flowering (days)	49.3±2.3	45.4±2.0 ^a	44.9±2.2 ^a	51.0±1.5	50.8±1.9	10
Lateral branches	1.6±0.7	4.7±0.9 ^a	4.4±1.0 ^a	1.2±0.6	4.2±1.9 ^a	10
Spikes	0±0	32.7±10.1 ^a	20.3±8.4 ^a	2.3±0.6 ^a	43.3±10.8 ^a	3
Leaf size (cm ²)	66±8	53±11 ^a	29±7 ^a	76±19	76±13	3
Epidermal Leaf cells (Nr.mm ⁻²)	399±76	492±42	444±12	443±11	362±50	3

^aValues significantly different from wild type (*P* < 0.05).

medium inhibited root growth in control and *orf13*-expressing plants in a similar way (data not shown).

Cytokinins are known to retard senescence (Gan and Amasino, 1995; Quirino et al., 2000). To further test the hypothesis that ORF13 interferes with cytokinin homeostasis, effects of *orf13* expression on senescence in tomato leaves were studied. No differences of protein and chlorophyll degradation were observed in plants expressing *orf13* or *orf13** compared to controls (data not shown).

Shoots or roots can be regenerated from leaf discs when cultivated on appropriate concentrations of auxin and cytokinin. The addition of auxin favors root production, whereas cytokinins induce callus and shoot growth (Skoog and Miller, 1957). In the absence of hormones, no growth of roots, callus, or shoots was observed, whereas in the presence of cytokinin, callus was formed on leaf discs of controls and the transgenic lines (data not shown). When auxin was added to the culture medium, control and *orf13** leaf discs formed roots, whereas in *orf13* leaf discs, root formation was repressed and occasionally callus growth was observed (Fig. 3C). The formation of roots increased with the auxin concentration present in the medium, but *orf13* lines always had reduced induction of root formation compared to controls and *orf13** lines. Since there was no callus growth on *orf13* leaf discs in the absence of hormones, cytokinin biosynthesis and signal perception seem not to be stimulated by the expression of *orf13*. However, root formation was reduced. Thus, *orf13* expression seems to inhibit root formation on leaf discs by acting on auxin perception or signaling. The fact that *orf13** leaf discs formed roots as control plants suggests that RB has regulatory functions in the formation of roots on leaf discs.

Effects of ORF13 on Cell Cycle Control

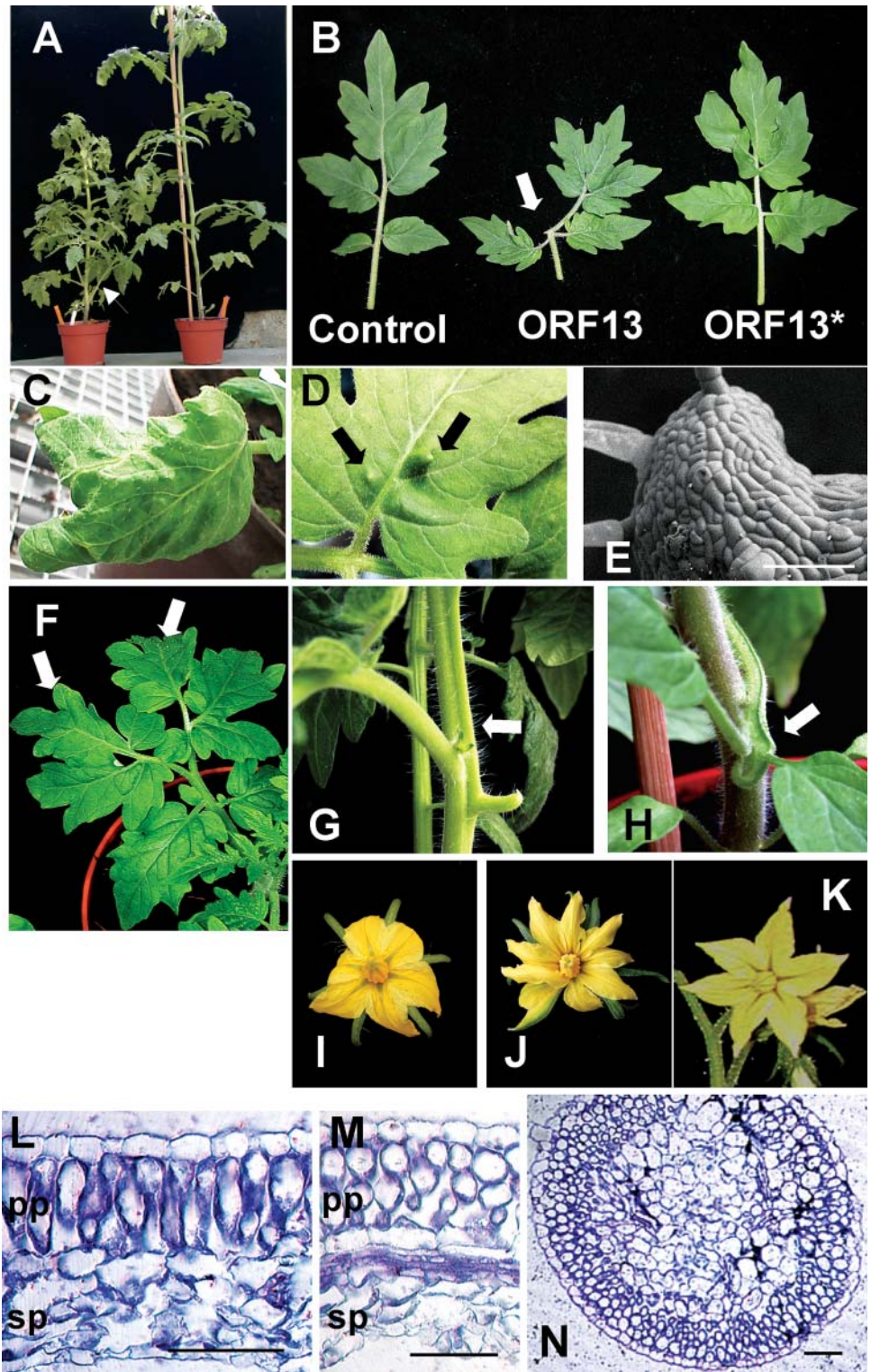
To test the hypothesis that ORF13 might interact with cell cycle regulation, the mitotic index of the shoot apical meristem (SAM), as well as the rate of leaf

primordium production, was determined. In addition, expression levels of several cell cycle genes were measured in expanded leaves by semiquantitative reverse transcription (RT)-PCR.

The structure of the SAM was not changed in *orf13*-expressing plants and layer organization was not disturbed (Fig. 4, A and B). Meristem diameter and cell size were comparable between transgenic and control plants (Table II). In plastic sections, mitotic figures were frequently observed in meristems of *orf13*-expressing plants (Fig. 4C). *Orf13*-expressing SAMs, but not *orf13** SAMs, had an increased mitotic index (Table II). The expression pattern of *histone H4* in meristems and young leaf primordia was visualized by in situ hybridization techniques. The intensity of staining for *histone H4* expression (marker for the S phase of the cell cycle) was increased in the vegetative meristem as well as in young primordia when the *orf13* gene was expressed (Fig. 4, D and E). In culture, *orf13*-expressing meristems formed more leaf primordia in 8 d than controls and *orf13** plants (Table II). Taken together, ORF13, but not ORF13*, had a positive effect on the rate of cell divisions in the SAM and on leaf formation.

To test the influence of *orf13* expression on the cell cycle activity in differentiated cells, the relative abundance of expression of several genes involved in cell cycle control was measured in the terminal leaflet of the second leaf of 3-week-old plants. The mRNA of *RB*, *E2F*, *cyclinD3.1*, *cyclinD3.3*, and *histone H4* were elevated when *orf13* was expressed compared to control plants, whereas expression levels of the small subunit of Rubisco (*rbcS*) and of *rpl2*, as well as total RNA contents, were comparable in control and *orf13* plants (Fig. 4F). Elevated contents of the mRNA of the cell-cycle-regulating genes were also observed in *orf13**, although the increase was stronger in *orf13*. These data suggest a higher cell division activity in cells of expanding leaves in the presence of *orf13* expression. Whereas an increase of *E2F*, *cyclinD3.1*, and *histone H4* mRNA suggest a higher cell cycle activity, elevated *RB* expression is expected to be found in cells of

Figure 2. Phenotype of tomato plants expressing the *A. rhizogenes* gene *orf13*. A, Size and shape of *orf13* (left) and wild-type tomato plants 51 d after sowing. The arrow points to a side branch of the *orf13*-expressing plant. B, Leaf architecture of wild-type, *orf13*, and *orf13** tomato leaves (arrow points to an outgrowth of the rachis). C, Wrinkled leaflet of an *orf13*-expressing plant. D, Spike formation on the adaxial side of *orf13* leaflets (arrow). E, SEM picture of rachis outgrowth at the place of the terminal leaflet in *orf13* plants. F, Leaf architecture of an *orf13*-expressing leaf (arrows point to the terminal leaflets). G, Fasciation of the stem (arrow) in *orf13* plants. H, Fusion of the petiole to the main stem (arrow) in *orf13* plants. I, Architecture of a wild-type flower. J, Architecture of an *orf13* flower. K, Architecture of an *orf13** flower. L, Transverse section of a wild-type leaf. M, Transverse section of an *orf13* leaf at the side of spike formation. N, Transverse section through an *orf13* spike. pp, Palisade parenchyma; sp, spongy parenchyma. Bars represent 20 μ m.



differentiating tissue. The changes in *RB* levels, due to *orf13* expression, indicate a perturbation of its normal functioning. Elevated levels of *RB* expression were also observed in Arabidopsis plants overexpressing *cyclinD3.1* (Dewitte et al., 2003).

Mitotic activity in the division zone of the main root was visualized by expressing the *cyclinB1.1::GUS* construct, including a mitotic destruction box (Colon-Carmona et al., 1999) in control plants and *orf13*-expressing plants. β -Glucuronidase (*GUS*) activity is

only present in cells that are in the G2/M transition. High mitotic activity was present in the division zone of the root in control and *orf13*-expressing plants. The division zone was not enlarged or reduced in *orf13*-expressing roots (Fig. 4, G and H).

Effects of ORF13 on the Expression of KNOX Transcription Factors

The accumulation of nondifferentiated cells in the spikes of *orf13*-expressing plants led us to investigate the expression of several KNOX-class transcription

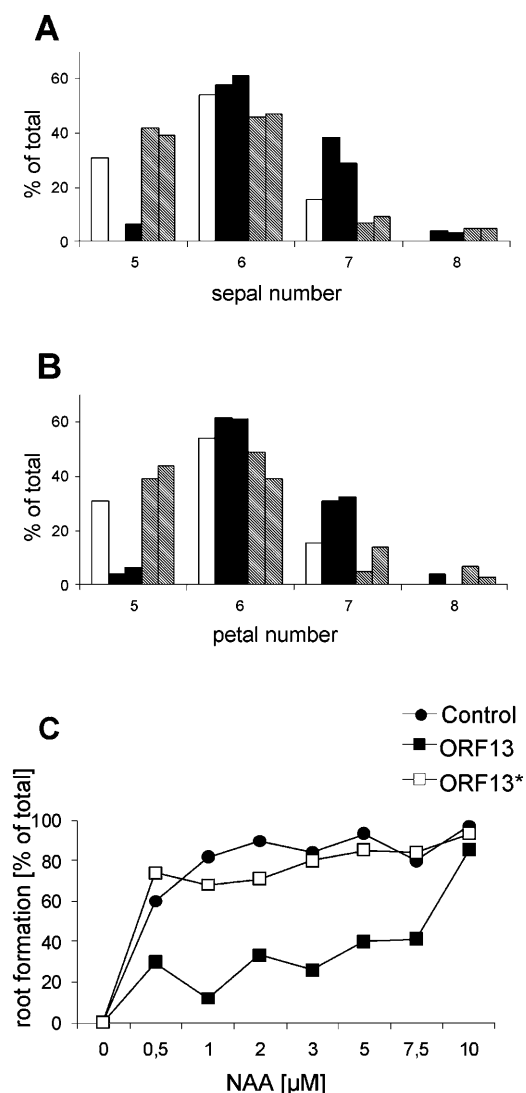


Figure 3. Influence of *orf13* expression on floral organ numbers and hormone homeostasis. Sepals (A) and petals (B) were counted of 20 flowers per plant ($n = 5$). For *orf13* and *orf13** lines, L1 and L2 were analyzed. White box, control; black box, ORF13; gray box, ORF13*. C, leaf discs ($n = 50$) of control, *orf13*- as well as *orf13**-expressing plants were incubated on MS medium containing 0, 0.5, 1, 2, 3, 5, 7.5, or 10 μ M NAA, and the leaf discs that had formed roots were counted after 10 d.

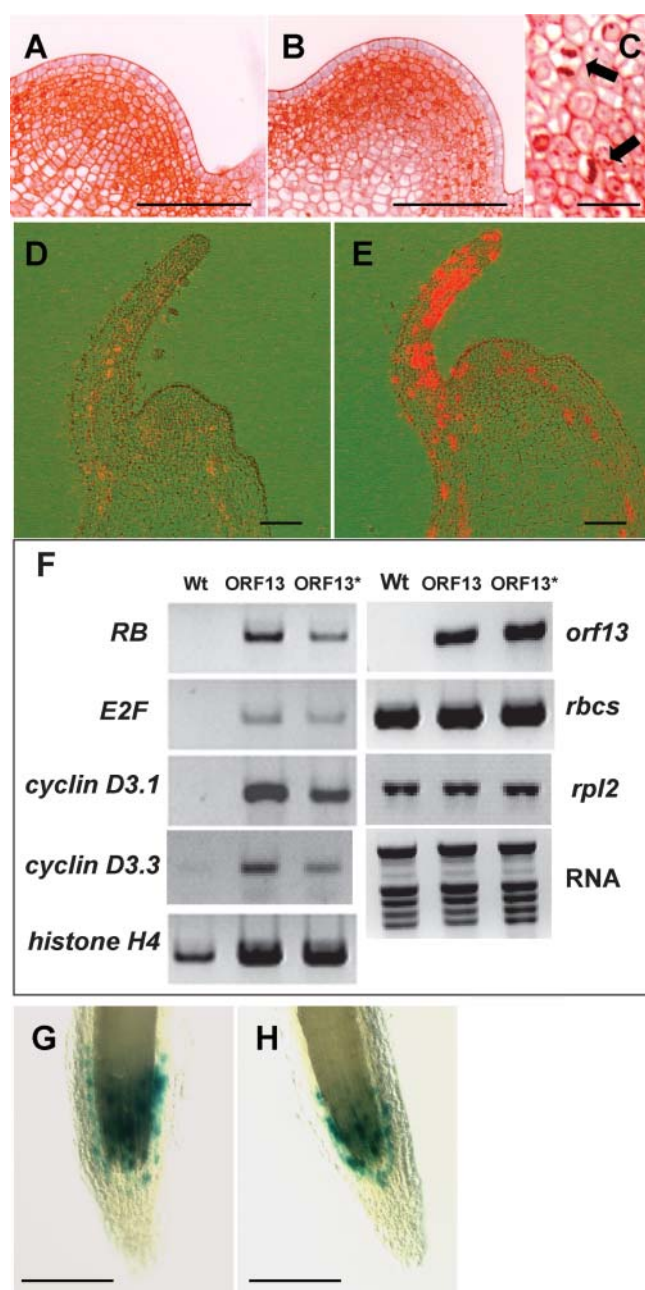


Figure 4. The influence of *orf13* expression on the cell cycle in the SAM, expanded leaves, and root meristems. A, SAM structure of a control and B, *orf13* 3-week-old vegetative meristem. C, Anaphase (arrow) in a vegetative meristem of an *orf13*-expressing plant. Sections were stained with DAPI and the colors of the pictures were inverted with a computer program. In situ localization of *histone H4* expression in the vegetative SAM of a 3-week-old wild type (D) and *orf13*-expressing (E) plant. Sections were hybridized with a *histone H4* antisense probe. F, Expression levels of cell cycle genes in the terminal leaflet of the second leaf of 3-week-old wild-type *orf13*- and *orf13**-expressing plants. Expression levels were determined by semiquantitative RT-PCR. RNA extraction and RT-PCR were repeated three times and each time showed similar expression patterns of the genes tested. G, *CyclinB1::GUS* expression in the division zone of a wild type; H, *orf13* main root. Bars represent 100 μ m, except in C, 10 μ m, and G and H, 200 μ m.

Table II. *Plastochron times, mitotic index, and meristem size of tomato plants expressing the A. rhizogenes gene orf13*

For plastochron determinations vegetative meristems were grown in culture and the formation of primordia was evaluated after an incubation time of 8 d ($n = 20$). For the determination of the mitotic index, epon sections ($5 \mu\text{M}$) of vegetative meristems were stained with DAPI and ana- and telophases were counted. Mean values \pm SD per section are shown for wild type ($n = 3$), ORF13 ($n = 5$), and ORF13* ($n = 4$) meristems. The size of the meristem was measured in the epon sections and cells were counted. All values were compared with values for the wild type using a one-tailed Student's *t* test. Values significantly different from wild type are reported with ^a ($P < 0.05$).

	Wild Type	ORF13	ORF13*
Cells (Nr 0.01 mm^{-2})	154 \pm 10.5	158 \pm 19.3	146 \pm 9.7
Nr. of primordia/8 d	4.2 \pm 0.76	5.4 \pm 0.50 ^a	4.1 \pm 0.46
Mitotic index	1.18 \pm 0.20	2.05 \pm 0.41 ^a	1.15 \pm 0.19
Size (μm)	156 \pm 9.3	159 \pm 11	150 \pm 2.7

factors. The class I KNOX transcription factors *LeT6* and *TKN1* are normally restricted to the SAM and to young leaflet primordia (Hareven et al., 1996; Chen et al., 1997; Reinhardt et al., 2003), whereas class II KNOX transcription factors display a broader expression pattern. *LeT6* was expressed in a similar pattern in wild-type and *orf13* meristems, although the labeling was stronger in *orf13*-expressing meristems (Fig. 5, A–C). In young leaf primordia, *LeT6* expression was minimal in control and *orf13* plants. When serial sections were analyzed, down-regulation of *LeT6* expression at the periphery of the meristem was observed, corresponding with the position of I_1 (Fig. 5C). This observation was made for control and *orf13* plants (data not shown for controls). This pattern of expression has been described for *STM*, which is only expressed in the meristem and not in young leaf primordia and is absent in the meristem, where a new primordium is initiated (I_1 ; Long et al., 1996; Lincoln et al., 1994). In control plants, *LeT6* mRNA was still detectable in the terminal leaflet of the second leaf of 21-d-old plants, but hardly detectable in leaves of 28-d-old plants. In contrast to that, in leaves expressing *orf13* or *orf13**, *LeT6* mRNA was detected abundantly in 21- and 28-d-old plants (Fig. 5E). *LeT6* expression was also detected in spikes (data not shown). *TKN1* expression, however, was not detected in leaves of control and *orf13* plants (Fig. 5E). The class II KNOX transcription factors *LeT12* and *TKN4* were both more abundant in leaves of *orf13* and *orf13** plants (Fig. 5E). These data show that ectopic expression of several KNOX genes was induced by ORF13 and was not dependent on a functional RB-binding site in ORF13.

DISCUSSION

We have investigated the influence of ectopic *orf13* expression on tomato plant growth, focusing on cell cycle control and KNOX-class transcription factor regulation. It has previously been proposed that *orf13*

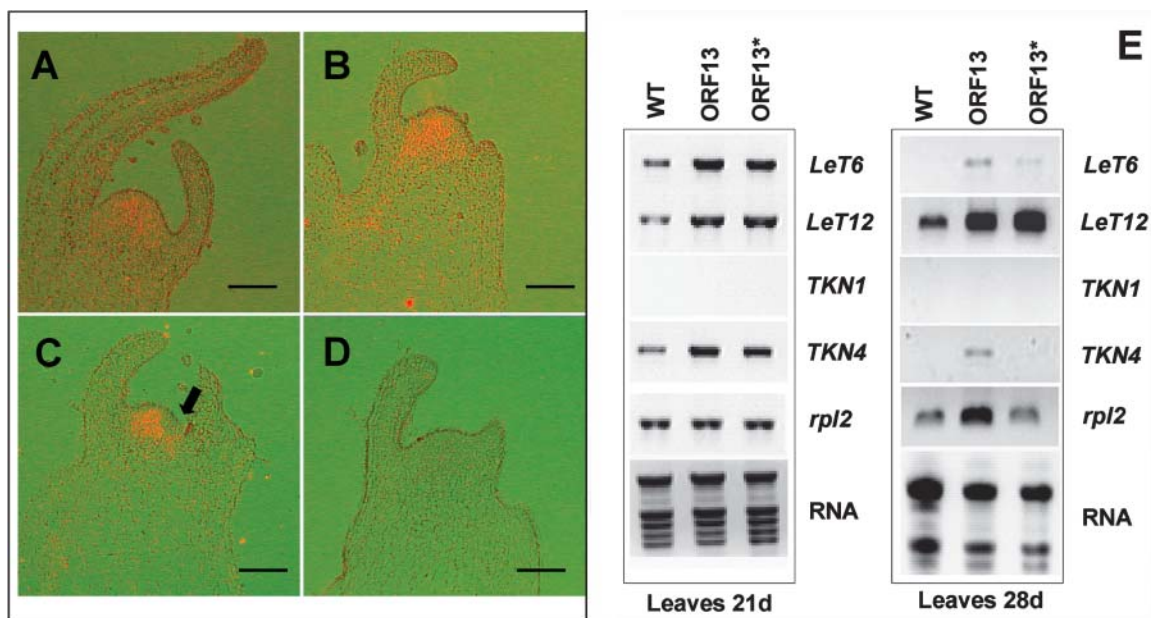
encodes a growth regulator that shares properties with cytokinins (Hansen et al., 1993), but divergent results were also obtained, where a hormone-related biochemical function for the *orf13* gene product was excluded (Lemcke and Schmülling, 1998). We have shown that ORF13 has an RB-binding motif and binds to RB in vitro (Fig. 1). Comparison of the phenotype of plants ectopically expressing the *orf13* gene to plants expressing *orf13** led us to conclude that several, but not all, developmental changes were due to a functional RB-binding motif in ORF13.

RB-Dependent Influence of *orf13* Expression

In our investigation, we were able to observe a proliferative effect of *orf13* expression in the SAM, where an increased number of mitoses was detected (Table II). This had no influence on meristem structure. In addition, the formation of leaf primordia was enhanced in *orf13*-expressing plants. The increased number of mitoses could be a consequence of the accumulation of cells in mitosis. Dewitte et al. (2003) observed accumulation of meristematic cells in the G2 phase of the cell cycle, when *cyclinD3.1* was ectopically expressed. In consequence, cell size, as well as meristem size, decreased and the formation of leaf primordia was retarded. In contrast, tobacco plants with ectopic expression of the *cyclinD2* gene had an accelerated growth rate, with no apparent differences in the size or structure of the SAM or meristematic cells. Growth rate increase was a consequence of a reduction of the length of the G1 phase and an increase in the number of cells entering the cell cycle (Cockcroft et al., 2000).

A smaller leaf size was observed in *orf13* but not in *orf13**-expressing plants. This is due to an earlier cessation of leaf growth and not to a reduced size of leaf cells, since the number of epidermal leaf cells per square millimeter was comparable to the number of cells in control and *orf13** leaves (Table I). Wyrzykowska et al. (2002) describe inhibitory effects of cell cycle activation by ectopic expression of *cyclinA3.2* on leaf growth. Aberrant leaf morphogenesis was also observed in Arabidopsis plants with ectopic expression of the *E2F-DP* transcription factor (De Veylder et al., 2002), as well as ectopic expression of *cyclinD3.1* (Dewitte et al., 2003).

Coordinated plant development requires controlled interaction of cell growth, cell division, and cell differentiation. Cell differentiation is often accompanied by a reduction of division activity. The cyclinD/RB/E2F pathway has been proposed to regulate the timing of cell cycle exit in relation to cell differentiation (de Veylder et al., 2002; Dewitte et al., 2003). As shown by Cockcroft et al. (2000), overall plant growth rates seem to be directly linked with cell division rates in the meristem and to have no influence on architecture and organ morphology. On the other hand, uncoupling of cell division and cell differentiation in developing organs leads to aberrant organ formation (De Veylder



F

	Control	ORF13	ORF13*
<i>rbcS</i>	1.0	0.89	1.38
<i>LeT6</i>	0	1.24	1.71
<i>orf13</i>	0	0.034	0.058

Expanded leaves of 4 week old tomato plants were used. Relative expression levels of *LeT6* and *orf13* were normalised to the corresponding plasmids and for *rbcS* expression levels, the wild type content was set to 1.

Figure 5. Influence of ORF13 on the expression pattern of KNOX-class transcription factors. A, In situ localization of *LeT6* in the vegetative meristem of a wild type; B and C, *orf13*-expressing plants. Sections were hybridized with a *LeT6* antisense probe. The arrow in C points to the down-regulation of *LeT6* expression at l_1 . D, Section of a wild-type vegetative meristem was hybridized with a *LeT6* sense probe. Bars represent 100 μ m. E, Expression levels of *LeT6*, *LeT12*, *TKN1*, *TKN4*, and *rpl2* in the terminal leaflet of the second leaf 21 and 28 d after sowing. Expression levels were determined by semiquantitative RT-PCR. F, Quantitative RT-PCR of *LeT6*, *rbcS*, and *orf13* in the terminal leaflet of the second leaf 28 d after sowing.

et al., 2002; Wyrzykowska et al., 2002; Dewitte et al., 2003). We propose that ORF13 interacts with the RB-protein through the LxCxE binding domain. In the SAM, this leads to an increased number of cell divisions and to an enhanced production of leaf primordia. In developing leaves, the interference of ORF13 with cell cycle regulation directs an earlier stop in organ growth. Furthermore, earlier flowering of *orf13*-expressing plants might restrain leaf initiation and leaf expansion, explaining the fewer leaves formed in *orf13* plants.

RB-Independent Effects of *orf13* Expression

Ectopic expression of the KNOX-class transcription factors *LeT6*, *LeT12*, and *TKN4* was observed in leaves

of *orf13*- and *orf13**-expressing tomato plants, suggesting a non-RB-dependent influence of *orf13* on KNOX gene expression (Fig. 5). The same was true for the formation of spikes, stunted growth, loss of apical dominance, fusion of organs, and stem fasciation. We interpret these changes to be a consequence of ectopic expression of KNOX genes. A relationship between KNOX gene expression and cytokinin contents was shown. Overexpression of KNOX genes increased cytokinin levels in different plant species (Kusaba et al., 1998; Hewelt et al., 2000; Frugis et al., 2001). On the other hand, plants with increased levels of cytokinins had enhanced expression of KNOX mRNA (Rupp et al., 1999). We have performed several bio-assays to analyze the influence of ORF13 on cytokinin and auxin homeostasis (data not shown). Except for

a reduced responsiveness of root formation on leaf discs incubated in the presence of auxin (Fig. 3C), no effects of *orf13* expression were observed in the bioassays. Therefore, we propose that the cytokinin-like phenotype observed in *orf13*-expressing plants is caused by ORF13 acting on KNOX expression and cell cycle regulation.

Role of ORF13 in Plant Infection

A. rhizogenes generates its living environment by changing the genetic program of infected plant cells, which start to produce nutrients for the bacteria and develop adventitious roots. The genetic program change is encoded on the bacterial T-DNA and has to be integrated into plant cells and replicated therein. For plant geminiviruses, an efficient method was described to subvert host cell cycle machinery and facilitate their replication (Gutierrez, 2000). The wheat dwarf virus synthesizes a replicase protein, RepA, which binds to the plant RB protein through the LxCxE binding motif, in order to activate cell replication and thus the replication of the viral genome (Kong et al., 2000). The sequence of the ORF13 protein contains the RB-binding site LxCxE and may have similar functions as RepA. The formation of roots from infected cells is more likely regulated by *rolA*, *rolB*, and *rolC*. Inactivation of *rolA* leads to an alteration of hairy root morphology, inactivation of *rolC* to reduced root formation, and inactivation of *rolB* to the abolition of virulence (White et al., 1985). The ectopic expression of *rolB* and, to a lesser extent, *rolA* and *rolC* are sufficient for the induction of hairy roots on the host plant. On the other hand, ectopic expression of other genes encoded on the T-DNA is not sufficient for root induction (Meyer et al., 2000). Infected plant cells have to be competent for a new differentiation program. This might be achieved by inducing a dedifferentiation program via the expression of KNOX-class transcription factors. We conclude that by converting differentiated cells into a dedifferentiation program, ORF13 acts in an RB-independent way on plant cells, whereas by activating cell divisions, ORF13 acts in an RB-dependent way. The function of ORF13 during *Agrobacterium* infection is to initiate a dedifferentiation program in differentiated plant cells and to activate cell divisions for replication of the T-DNA.

MATERIALS AND METHODS

Cloning of the *orf13* Gene and Mutagenesis

The full-length *orf13* was amplified by PCR from pRi8196 (accession no. M60490; Hansen et al. 1991) using primers 5' AAATGGATCCATGGCTCGTTC and 5' GATGCGAATTCTATTGGAGC and introducing a *Bam*HI and an *Eco*RI site on the 5' and 3' ends, respectively. The fragment was cloned into pBluescript (SK-; Stratagene, La Jolla, CA) leading to pBSorf13. The *Bam*HI-*Hind*III *orf13* fragment was excised from pBSorf13 and ligated into the 6-His tag expression vector pQE30 (Qiagen, Valencia, CA), leading to pQE30orf13. Mutagenesis of the LxCxE motif in the ORF13 protein, C101A, and E103K was carried out with the primer 5'-GGAGACAAGCAC-

TCTTGGCCAAAAAGATTCGGATGG-3' and its complement using the QuickChange Site-Directed mutagenesis kit (Stratagene), according to the manufacturer's instructions, creating pQE30ORF13LAK. The fragments containing the ORF from both pQE30ORF13 and pQE30ORF13LAK were excised from pQE30 with *Bam*HI and *Hind*III and ligated into pBluescript, reexcised with *Bam*HI-*Kpn*I, and ligated into pBi121Gd leading to pBi121ORF13LCE (*orf13*) and pBi121ORF13LAK (*orf13**), respectively. The plasmid pBi121Gd was derived from pBi121 (CLONTECH, Palo Alto, CA) by replacing the *uidA* gene (GUS) with the *Xba*I-*Sst*I fragment from pUC18 (CLONTECH).

Plant Transformation

PBi121ORF13LCE and pBi121ORFLAK were introduced into *Agrobacterium tumefaciens* strain LBA4404. For plant transformation, cotyledon leaf discs of tomato plants (*Lycopersicon esculentum* cv MoneyMaker) were soaked in YEB solution containing the transgenic *A. tumefaciens* for 1 min and then transferred to plates containing 1× Murashige and Skoog (MS) medium, 3% Suc, 1× vitamin B5, pH 5.8, 8% agarose (MS medium) supplied with 120 μg L⁻¹ naphthalene-L-acetic acid (NAA) and 1 mg L⁻¹ 6-benzylaminopurine, and were incubated in the dark for 48 h. Then leaf discs were transferred to MS medium containing zeatin (2 mg mL⁻¹) at 18-h-light, 6-h-dark cycles at 23°C. When shoots emerged from leaf discs, they were transferred to MS medium lacking zeatin for rooting. Appropriate antibiotics were added to growing media for the selection of the integrated gene.

Tomato plants were also transformed with the *cyclinB1.1::GUS* construct (Colon-Carmona et al., 1999) as described. Homozygous *orf13* plants were crossed to homozygous *cyclinB1.1::GUS* plants. For analysis, plants were selected homozygous for *orf13* and *cyclinB1.1::GUS*.

Plant Growth and Phenotype Description

Tomato plants were grown in soil (16-h-light, 8-h-dark cycles, at 25°C and 60% humidity). Pictures were taken with a Nikon (Tokyo) digital camera (Coolpix 5000). Scanning electron microscopy (SEM) pictures were made with a variable-pressure scanning electron microscope (model S-3500 N; Hitachi, Tokyo). Leaf area of the third leaf of 3-week-old plants was measured with an area meter (DELTA-T DEVICES). For analyses of epidermal leaf cells, the adaxial side of the terminal leaflet of the third leaf from the bottom 28 d after sowing was visualized by SEM and cells were counted. Plastic sections were prepared as described previously (Loreto et al., 2001), with one modification: OsO₄ was omitted. Semithin sections (5 μm) were stained with toluidine blue (0.1%) or 4',6-diamidino-2-phenylindole (DAPI) and viewed on a Zeiss (Jena, Germany) Axioskop2 equipped with an AxioCam camera. The mitotic index was determined by counting ana- and telophases of consecutive meristem semithin sections (5 μm) stained with DAPI. Pictures of sections stained with DAPI were inverted with Photoshop for clarity. Cells of the meristem were counted on the semithin sections and the diameter of the meristem was determined.

In Vitro Culture, Auxin Responsiveness, and GUS Histochemical Assay

For tissue culture experiments, primary leaves of tomato plants were sterilized (ethanol 70% for 1 min, bleach for 7 min) and leaf discs were incubated on plates containing MS medium with different concentrations of hormones added to the medium (NAA, 0–10 μM, zeatin, 0–10 μM). Leaf discs that had formed callus or roots were counted 10 d after incubation.

For the GUS histochemical assay, roots were prefixed in 50 mM NaPO₄, pH 7.0, containing 8% (v/v) formaldehyde and 0.25% (v/v) glutaraldehyde for 45 min and incubated in staining solution (50 mM NaPO₄, pH 7.0, 0.5 mg mL⁻¹ X-gluc, 1 mM K₄Fe(CN)₆, and 1 mM K₃Fe(CN)₆) for 10 to 16 h at 37°C. GUS staining was visualized with a Sony (Tokyo) camera attached to a Nikon microscope.

In Situ Hybridization Analysis

Tissue fixation, sectioning, and in situ hybridization with the *histone H4* and *LeT6* probes were as described by Fleming et al. (1993). Signals were visualized through a polarizing filter set with epifluorescent illumination and the silver particles were rendered red and superimposed on a bright-field

image of the section. No substantial signal above background was apparent after hybridization with sense probes.

RNA Extraction, Reverse Transcription, and PCR

RNA of expanded leaves of 3- and 4-week-old plants was extracted as described by Caderas et al. (2000). Total RNA (1 µg) was DNase I treated. First-strand synthesis of cDNA was performed by using oligo(dT) primer and avian myeloblastosis virus RT. The following primers were used for RT-PCR experiments: *E2F* (accession no. TC105867) 5'-CCATATGCCTAAACTTCAAGA and 5'-GGAGTCTTCAACAATTCCA, *cyclinD3.1* (accession no. CAB51788) 5'-GATGGCCTTACTGTGAGGA and 5'-GCAACAGCAGCAAGCTGACT, *rbcs* (accession no. X05983) 5'-AATGGATGGGTTCTTGCTTGG and 5'-TGCCCTAAAGACAATTTTGTCC, *cyclinD3.3* (accession no. AJ002590) 5'-CATCTGCCACAATGTTGCATGT and 5'-TGACTCCCTAATCTTCTTGGAC, *LeT6* (accession no. AF000141) 5'-GCACTAGATCAGTTCATGAGGC and 5'-GGATGAGCAGCATCCATCACAAC, *histone H4* (accession no. X69179) 5'-ATGTCTGGTCGTGAAAGGGAG and 5'-GATCTAAGCCATAAGAACAGCAC, *LeRb* 5'-CGATGACAACTGCCAGGTGGCTGC and 5'-GTAAGTCTTGTGAGTGCAA, *orf13* 5'-AGAGGCTGCCTATGTCAAC and 5'-TATTCACGACGACCTTGC, *rpl2* 5'-GGTCGTGTATCAGAGCAC and 5'-GATAACAATGGCGTAATCACC, *TKN1* 5'-TATGCTTGGAATGCTCCCGTTCC and 5'-GTGACCTTCCATATAAAGAGCAGC, *LeT12* 5'-ACAAAGCTTAACAGGGGTAGCACC and 5'-GTGGTCAATTACTTCCACAGCCA, *TKN4* 5'-CAGCTCAGTTCCTATGCAAA and 5'-GATCCAGCACTTACACCTTCCA. Annealing temperatures for *E2F* primers was 53°C, for *orf13* and *rpl2* primers, 55°C, for *cyclinD3.1* and *cyclinD3.3* primers, 57°C, for *histone H4* and *LeRb* primers, 58°C, and for *LeT6*, *TKN1*, *TKN4*, *LeT12*, and *rbcs* primers, 62°C, and 42 cycles were used to amplify the cDNA. Quantitative real-time PCR measurements for *rbcs*, *LeT6*, and *orf13* were carried out as described in Kürsteiner et al. (2003).

Cloning of a Partial cDNA of Tomato RB

Synthesis of cDNA from tobacco leaf RNA was performed as described. Degenerate primers for the RB sequence were designed (FW: 5'-TGTAAGCACAGCGATGACAAC, REV: 5'-GTACATTGAAGATCCTTTTCCCA), and PCR was carried out with tobacco cDNA. The resulting fragment was purified (NucleoSpin Extract, Marcherey-Nagel, Duren, Germany), cloned into pBluescript SK (-), and sequenced. The resulting sequence (5'-AATTGGTACCCGGGCCCCCTCGAGGTCGACGGTATCGATAAGCTTGATTGTAAAGCACAGCGATGACAACACTGCCAGGTGGCTGCGTACCGTCATAGCTCACTACAGGCAAAACCTTACCTGAGTGGAGAGATTTTTGTCTGCCTGTGATAGGAATGTATCAGCTGATGTATCCGGAGGGCTCACATTATCTGGAGCTATATTTCCAAGTAGTGGTCTGGGGAGCATTGTGGCGCTGGGAGCCTGCAAAAGCACAAGCTTAATGGACAACATATGGCAGAGCAACGCTAGATCTGAGTCTCTGAAGTTGTATTATAGGGTCTCGACAGATGTGTGTCGAGAATCTCAGATTTGCATGTGACCAATTAACCTCGTTGCTAACCAATGAGAGGTTTCATAGATGTATGCTTGCCTGTCCAGCTGAACACTAGTTCTTGCCACTCACAAGCAGTTACAATGTTTCCAGCTGTGTTTGGAGAGAACAGGAATTACCTTTTGTATCTCAGTAAGGTGATAGAGAGCCTTCATCAGGCATGAAGAAAGTCTTCCCTCGAGAAGTGTAGACGCCATTGGAATCACTCGAAGAAAGACTCTGGAGAGCATGGTTTG) has 91% identity to NtRb1 (accession no. AB015221).

Pull-Down Assays

Recombinant proteins were produced in *Escherichia coli* strain M15 (Qiagen) and the pull-down assay performed according to the procedure of Groisman and collaborators (Groisman et al., 1996) with modifications. The plasmids pGEXRb and pGEXRb(C706F) carrying constructs for the expression of the amino acids 379 to 928 of the human pRb as an N-terminal GST fusion (Kaelin et al., 1991) were a kind gift from Didier Trouche (Institut Gustave Roussy, Villejuif, France). Bacterial cultures were inoculated with an overnight preculture at a one-fifteenth dilution in Luria-Bertani broth and incubated at 28°C for pQE30ORF13 constructs and at 37°C for the pGEXRb constructs. Once an OD₆₀₀ of 0.6 to 0.8 was reached, protein production was induced with 40- and 100-µM isopropylthio-β-galactoside for 6-His-pORF13 and GST-pRb, respectively. Aliquots of 100-mL culture were pelleted and resuspended with 2 mL NETN (100 mM NaCl, 1 mM EDTA, 20 mM Tris-HCl, pH 8.0, 0.5% [v/v] Nonidet P-40), 1 mM DTT, 1 mM PMSF, 0.1 KI units aprotinin (Calbiochem-Novabiochem, San Diego, CA; pORF13), and 5 mL

NETN (pRb). Bacteria were lysed by sonication (3 min at the power 5–6, 50% duty cycle, VibraCell, Sonics & Materials, Newtown, CT) and the debris pelleted at 48,000g, 30 min. The supernatant containing the GST-pRb fusion proteins was incubated for 2 h at 4°C with 100 µL glutathion-4B-Sepharose beads (Pharmacia, Piscataway, NJ) equilibrated with NETN. The coated beads were then gently centrifuged at 700g, washed twice with NETN, and incubated for 4 h at 4°C with the supernatants containing the 6-His-ORF13 fusion proteins. Subsequently, the protein complexes attached to the beads were collected by gentle centrifugation at 700g, washed three times with NETN, and denatured by the addition of 1 volume 2 × SDS gel loading buffer. Input control samples were collected from the supernatants following the sonifications. SDS-PAGE was performed on 10% gels according to the protocol of Laemmli et al. (1970) adapted for slab gels. Proteins were transferred to nitrocellulose membranes (Schleicher & Schüll, Keene, NH) and decorated with either anti-Rb monoclonal antibodies (PharMingen, San Diego) or monoclonal antibodies against N-terminal 6-His tags (Qiagen) followed by goat anti-mouse alkaline phosphatase conjugates (Sigma-Aldrich, St. Louis). Alkaline phosphatase was revealed with NBT and BCIP (Sigma-Aldrich) in 100 mM NaCl, 5 mM MgCl₂, Tris-HCl, pH 9.5.

Sequence data from this article have been deposited with the EMBL/GenBank data libraries under accession numbers M60490, TC105867, CAB51788, X05983, AJ002590, AF000141, X69179, AB015221, X64562, U32247, AF000142, and AF533597.

ACKNOWLEDGMENTS

We thank Therese Mandel (Institute of Plant Sciences, University of Bern, Switzerland) for technical support and Peter Doerner (Salk Institute for Biological Studies, La Jolla, CA) for the *cyclinB1::GUS* construct. We also thank Thomas Schmülling (Institute of Biology/Applied Genetics, Freie Universität Berlin, Germany), Samuel Zeeman and Didier Reinhardt (both Institute of Plant Sciences, University of Bern, Switzerland) for critical reading of the manuscript, and our colleagues in the laboratory for stimulating discussions.

Received February 12, 2004; returned for revision April 26, 2004; accepted May 2, 2004.

LITERATURE CITED

- Aoki S, Kawaoka A, Sekine M, Ichikawa T, Fjita T, Shinmyo A, Syono K (1994) Sequence of the cellular T-DNA in the untransformed genome of *Nicotiana glauca* that is homologous to ORFs 13 and 14 of the Ri plasmid and analysis of its expression in genetic tumors of *N. glauca* × *N. langsdorffii*. *Mol Gen Genet* 243: 706–710
- Caderas D, Muster M, Vogler H, Mandel T, Rose JKC, McQueen-Mason S, Kuhlemeier C (2000) Limited correlation between expansin gene expression and elongation growth rate. *Plant Physiol* 123: 1399–1413
- Celenza JL, Grisafi PL, Fink GR (1995) A pathway for lateral root formation in *Arabidopsis thaliana*. *Genes Dev* 9: 2131–2142
- Chen J-J, Janssen B-J, Williams A, Sinha N (1997) A gene fusion at a homeobox locus: alterations in shape and implications for morphological evolution. *Plant Cell* 9: 1289–1304
- Chuck G, Lincoln C, Hake S (1996) KNAT1 induces lobed leaves with ectopic meristems when overexpressed in *Arabidopsis*. *Plant Cell* 8: 1277–1289
- Cockcroft CE, den Boer BGW, Healy JMS, Murray JAH (2000) Cyclin D control of growth rate in plants. *Nature* 405: 575–579
- Colon-Carmona A, You R, Haimovitch-Gal T, Doerner P (1999) Spatio-temporal analysis of mitotic activity with a labile cyclin-GUS fusion protein. *Plant J* 20: 503–508
- Davies PJ (1995) The plant hormones: their nature, occurrence and functions. In PJ Davies, ed, *Plant Hormones: Physiology, Biochemistry and Molecular Biology*. Kluwer Academic, Dordrecht, The Netherlands, pp 1–12
- De Veylder L, Beeckman T, Beemster GTS, Engler JDA, Ormenese S, Maes S, Naudts M, Van Der Schueren E, Jacqumard A, Engler G, et al (2002) Control of proliferation, endoreduplication and differentiation by the *Arabidopsis* E2Fa-Dpa transcription factor. *EMBO J* 21: 1360–1368

- Dewitte W, Riou-Khamlichi C, Scofield S, Healy JMS, Jacqmar A, Kilby NJ, Murray JAH (2003) Altered cell cycle distribution, hyperplasia, and inhibited differentiation in *Arabidopsis* caused by the D-type cyclin CYCD3. *Plant Cell* **15**: 79–92
- Du W, Vidal M, Xie J-E, Dyson N (1996) RBF, a novel RB-related gene that regulates E2F activity and interacts with cyclin E in *Drosophila*. *Genes Dev* **10**: 1206–1218
- Estruch JJ, Schell J, Spena A (1991) The protein encoded by the *rolB* plant oncogene hydrolyses indole glucosides. *EMBO J* **10**: 3125–3128
- Fleming AJ, Mandel T, Roth I, Kuhlemeier C (1993) The patterns of gene expression in the tomato shoot apical meristem. *Plant Cell* **5**: 297–309
- Frugis G, Giannino D, Mele G, Nicolodi C, Chiappetta A, Bitonti MB, Innocenti AM, Dewitte W, Van Onckelen V, Mariotti D (2001) Overexpression of *KNAT1* in lettuce shifts leaf determinate growth to a shoot-like indeterminate growth associated with an accumulation of isopentenyl-type cytokinins. *Plant Physiol* **126**: 1370–1380
- Fründt C, Meyer AD, Ichikawa T, Meins F (1998) A tobacco homologue of the Ri-plasmid *orf13* gene causes cell proliferation in carrot root discs. *Mol Gen Genet* **259**: 559–568
- Gan S, Amasino RM (1995) Inhibition of leaf senescence by autoregulated production of cytokinin. *Science* **270**: 1986–1988
- Groisman R, Masutani H, Leibovitch MP, Robin P, Soudant I, Trouche D, Harel-Bellan A (1996) Physical interaction between the mitogen-responsive serum response factor and myogenic basic-helix-loop-helix proteins. *J Biol Chem* **271**: 5258–5264
- Gutierrez C (2000) DNA replication and cell cycle in plants: learning from geminiviruses. *EMBO J* **19**: 792–799
- Hansen G, Larribe M, Vaubert D, Tempe J, Biermann BJ, Montoya AL, Chilton MD (1991) *Agrobacterium rhizogenes* pRi8196 T-DNA: mapping and DNA sequence of functions involved in mannopine synthesis and hairy root differentiation. *Proc Natl Acad Sci USA* **88**: 7763–7767
- Hansen G, Vaubert D, Heron JN, Clerot D, Tempe J, Brevet J (1993) Phenotypic effects of overexpression of *Agrobacterium rhizogenes* T-DNA ORF13 in transgenic tobacco plants are mediated by diffusible factors. *Plant J* **4**: 581–585
- Hareven D, Gutfinger T, Parnis A, Eshed Y, Lifschitz E (1996) The making of a compound leaf: genetic manipulation of leaf architecture in tomato. *Cell* **84**: 735–744
- Hewelt A, Prinsen E, Thomas M, Van Onckelen H, Meins F (2000) Ectopic expression of maize *knotted1* results in the cytokinin-autotrophic growth of cultured tobacco tissues. *Planta* **210**: 884–889
- Horowitz JM, Yandell DW, Park SH, Canning S, Whyte P, Buchkovich K, Harlow E, Weinberg RA, Dryja TP (1989) Point mutational inactivation of the *retinoblastoma* antioncogene. *Science* **243**: 937–940
- Kaelin WG, Ewen ME, Livingston DM (1990) Definition of the minimal simian virus 40 large T antigen- and adenovirus E1A-binding domain in the *retinoblastoma* gene product. *Mol Cell Biol* **10**: 3761–3769
- Kaelin WG, Pallas DC, DeCaprio JA, Kaye FJ, Livingston DM (1991) Identification of cellular proteins that can interact specifically with the T/E1A-binding region of the *retinoblastoma* gene product. *Cell* **64**: 521–532
- Kelly MO, Bradford KJ (1986) Insensitivity of the *diageotropica* tomato mutant to auxin. *Plant Physiol* **82**: 713–717
- Kong L-J, Orozco BM, Roe JL, Nagar S, Ou S, Feiler HS, Durfee T, Miller AB, Grissem W, Robertson D, et al (2000) A geminivirus replication protein interacts with the *retinoblastoma* protein through a novel domain to determine symptoms and tissue specificity of infection in plants. *EMBO J* **19**: 3485–3495
- Kürsteiner O, Dupuis I, Kuhlemeier C (2003) The *pyruvate decarboxylase1* gene of *Arabidopsis* is required during anoxia but not other environmental stresses. *Plant Physiol* **132**: 968–978
- Kusaba S, Kano-Murakami Y, Matsuoka M, Tamaoki M, Sakamoto T, Yamaguchi I, Fukumoto M (1998) Alteration of hormone levels in transgenic tobacco plants overexpressing the rice homeobox gene *OSH1*. *Plant Physiol* **116**: 471–476
- Laemmli UK (1970) Cleavage of structural proteins during the assembly of the head of bacteriophage T4. *Nature* **227**: 680–685
- Lemcke K, Schmülling T (1998) Gain of function assays identify non-rol genes from *Agrobacterium rhizogenes* TL-DNA that alter plant morphogenesis or hormone sensitivity. *Plant J* **15**: 423–433
- Lincoln C, Long J, Yamaguchi J, Serikawa K, Hake S (1994) A knotted-like homeobox gene in *Arabidopsis* is expressed in the vegetative meristem and dramatically alters leaf morphology when overexpressed in transgenic plants. *Plant Cell* **6**: 1859–1876
- Long JA, Moran EI, Medford JI, Barton MK (1996) A member of the KNOTTED class of homeodomain proteins encoded by the STM gene of *Arabidopsis*. *Nature* **379**: 66–69
- Loreto F, Mannozi M, Maris C, Nascetti P, Ferranti F, Pasqualini S (2001) Ozone quenching properties of isoprene and its antioxidant role in leaves. *Plant Physiol* **126**: 993–1000
- Medford JI, Horgan R, El-Sawi Z, Klee HJ (1989) Alterations of endogenous cytokinins in transgenic plants using a chimeric isopentenyl transferase gene. *Plant Cell* **1**: 403–413
- Meyer A, Tempé J, Costantino P (2000) Hairy root; a molecular overview. Functional analysis of *Agrobacterium rhizogenes* T-DNA genes. In G Stacey, NT Keen, eds, *Plant Microbe Interactions*. APS Press, St. Paul, pp 93–139
- Mironov V, De Veylder L, Van Montagu M, Inzé D (1999) Cyclin-dependent kinases and cell division in plants: the nexus. *Plant Cell* **11**: 509–521
- Murray JAH (1997) The *retinoblastoma* protein is in plants. *Trends Plant Sci* **2**: 82–84
- Nilsson O, Olsson O (1997) Getting to the root: the role of the *Agrobacterium rhizogenes* *rol* genes in the formation of hairy roots. *Physiol Plant* **100**: 463–473
- Quirino BF, Noh Y-S, Himelblau E, Amasino RM (2000) Molecular aspects of leaf senescence. *Trends Plant Sci* **5**: 278–282
- Reinhardt D, Frenz M, Mandel T, Kuhlemeier C (2003) Microsurgical and laser ablation analysis of interactions between the zones and layers of the tomato shoot apical meristem. *Development* **130**: 4073–4083
- Reed RC, Brady SR, Muday GK (1998) Inhibition of auxin movement from the shoot into the root inhibits lateral root development in *Arabidopsis*. *Plant Physiol* **118**: 1369–1378
- Riou-Khamlichi C, Huntley R, Jacqmar A, Murray JAH (1999) Cytokinin activation of *Arabidopsis* cell division through a D-type cyclin. *Science* **283**: 1541–1544
- Rupp HM, Frank M, Werner T, Strnad M, Schmülling T (1999) Increased steady state mRNA levels of the *STM* and *KNAT1* homeobox genes in cytokinin overproducing *Arabidopsis thaliana* indicate a role for cytokinins in the shoot apical meristem. *Plant J* **18**: 557–563
- Sentoku N, Sato Y, Matsuoka M (2000) Overexpression of rice *OSH* genes induces ectopic shoots on leaf sheaths of transgenic rice plants. *Dev Biol* **220**: 358–364
- Sinha N, Williams R, Hake S (1993) Overexpression of the maize homeobox gene, *KNOTTED-1*, causes a switch from determinate to indeterminate cell fates. *Genes Dev* **7**: 787–795
- Skoog E, Miller CO (1957) Chemical regulation of growth and organ formation in plant tissues cultured in vitro. *Symp Soc Exp Biol* **11**: 118–131
- Slightom JL, Durand-Tardif M, Jouanin L, Tepfer D (1986) Nucleotide sequence analysis of the TL-DNA of *Agrobacterium rhizogenes* agropine type plasmid. *J Biol Chem* **261**: 108–121
- Weinberg RA (1995) The *retinoblastoma* protein and cell cycle control. *Cell* **81**: 323–330
- White FE, Taylor BH, Huffman GA, Gordon MP, Nester EW (1985) Molecular and genetic analysis of the transferred DNA regions of the root-inducing plasmid of *Agrobacterium rhizogenes*. *J Bacteriol* **164**: 33–44
- Wyrzykowska J, Pien S, Shen WS, Fleming AJ (2002) Manipulation of leaf shape by modulation of cell division. *Development* **129**: 957–964
- Zhu J, Oger PM, Schrammeijer B, Hooykaas PJJ, Farrand SK, Winans SC (2000) The bases of crown gall tumorigenesis. *J Bacteriol* **182**: 3885–3895
- Zobel RW (1974) Control of morphogenesis in the ethylene-requiring tomato mutant, *diageotropica*. *Can J Bot* **52**: 735–741
- Zupan J, Muth TR, Draper O, Zambryski P (2000) The transfer of DNA from *Agrobacterium tumefaciens* into plants: a feast of fundamental insights. *Plant J* **23**: 11–28